Rev.Adv.Mater.Sci. 18(2008) 476-480

COMPARISON OF NANOCRYSTALLINE FRACTIONS DETERMINED BY VARIOUS METHODS

K. Pękała[1], P. Jaskiewicz[1], A. Grabias[2] and J. Latuch[3]

[1]Faculty of Physics, Warsaw University of Technology, Koszykowa 75, 00-662 Warsaw, Poland
[2] Institute of Electronic Materials Technology, Wólczynska 133, 01-919 Warsaw, Poland
[3]Faculty of Materials Science and Engineering, Warsaw University of Technology, Woloska 141, 02-507 Warsaw, Poland

Received: March 29, 2008

Abstract. Various experimental methods are applied to evaluate the nanocrystalline fraction in $Fe_{87}Zr_7B_6$ alloys. These are: differential scanning calorimetry, electrical resistivity, Mössbauer spectroscopy and magnetization measurements. A comparison of the results obtained by the experimental methods applied and their experimental accuracy are presented. The influence of assumptions and simplifications inherent for different methods is described and discussed. Particular limitations and applicability ranges are analyzed.

1. INTRODUCTION

In many publications [1,2] a kinetics of nanocrystallization processes occurring in amorphous alloys is described by the crystalline volume fraction X determined by different methods. In this paper we show and discuss the temperature dependence of X fraction derived from experimental data of differential scanning calorimetry (DSC), electrical resistivity, Mössbauer spectroscopy and magnetization measurements.

2. EXPERIMENTAL DETAILS

Amorphous alloy $Fe_{87}Zr_7B_6$ was prepared by copper roller melt spinning method in argon atmosphere. The amorphicity of the samples was checked by means of X-ray diffraction (XRD). Transmission Mössbauer spectra were measured at room temperature using a 25 mCi ^{57}Co-in-Rh source. Magnetization was recorded as a function of temperature using the Faraday balance. Electrical resistivity was measured by the DC four probe method. The electrical resistivity and DSC and magnetization measurements were performed with the heating rate of 20 K/min. The samples for Mössbauer measurements were prepared by heating alloys with the same rate up to T_m =860, 880, 910K followed by a fast cooling down to the room temperature.

3. RESULTS AND DISCUSSION

3.1. Magnetization

The temperature dependence of magnetization of the amorphous $Fe_{87}Zr_7B_6$ alloy (Fig. 1) shows that a ferromagnetic ordering of the amorphous phase decays above 330K, which is in agreement with a report [3]. The magnetization increase observed at about 830K is due to a precipitation of bcc Fe nanograins with diameter below 20 nm [4].The APFIM (Atom Probe Field Ion Microscopy) results show that boron atoms remain in Fe grains, when Zr atoms are almost completely rejected [5]. The XRD spectra show that the increase of unit cell parameter of the bcc – Fe phase may be caused by the dissolved Zr and B atoms [6].

Corresponding author: Krystyna Pekala, e-mail: pekala@mech.pw.edu.pl

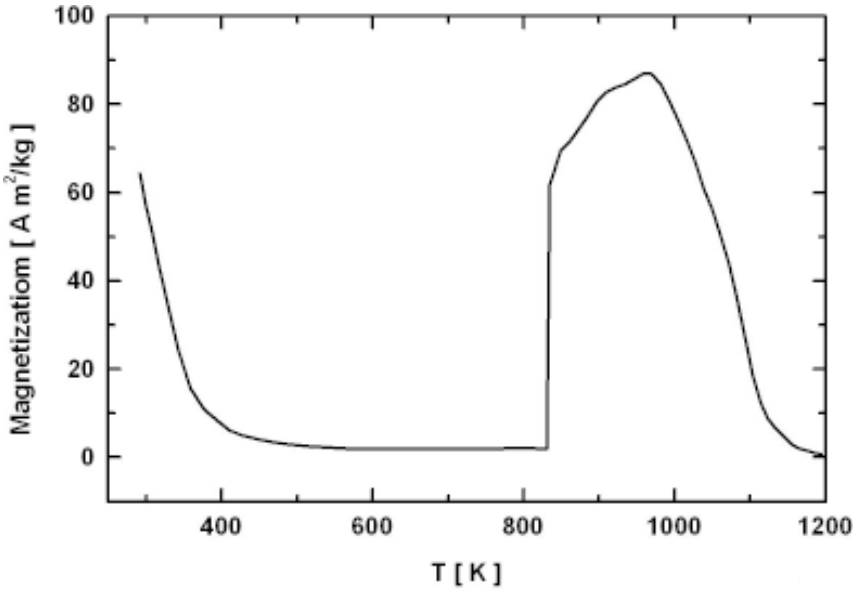

Fig. 1. Temperature dependence of magnetization for amorphous $Fe_{87}Zr_7B_6$ alloy.

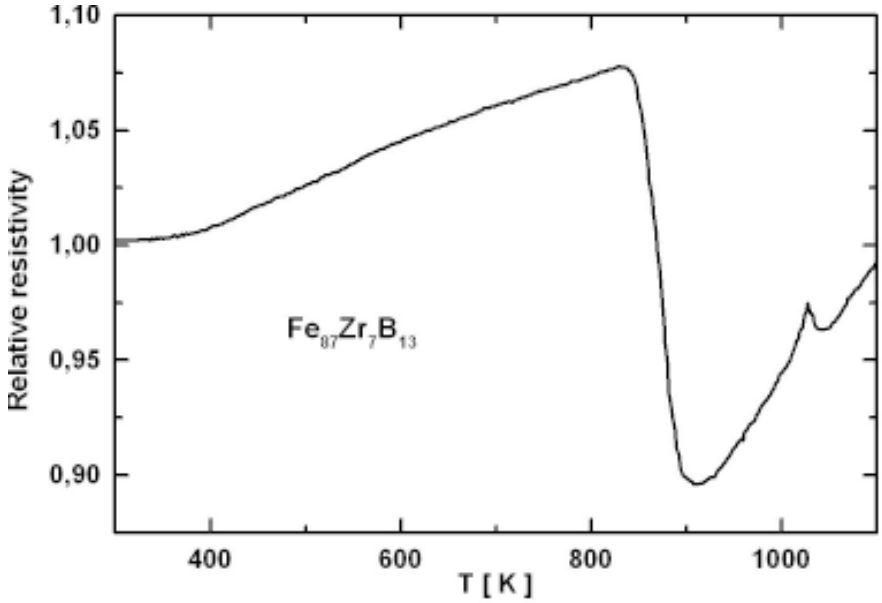

Fig. 2. Temperature dependence of electrical resistivity for amorphous $Fe_{87}Zr_7B_6$ alloy.

The volume fraction of the nanocrystalline phase was calculated using the formula:

$$X = \frac{M - M_a}{M_c - M_a}, \qquad (1)$$

where M_a, M_c are the magnetizations of the amorphous and nanocrystalline phases, respectively. M is the measured magnetization of the composite alloy composed of the nanocrystalline bcc Fe phase embedded in the amorphous matrix. In our calculations, we assume that the amorphous matrix is paramagnetic and that M_a is almost equal to zero. M_c is approximated by a magnetization of polycrystalline bcc - Fe according to Cullity [7]. The calculated values of $X(T)$ (Fig. 4) vary from 0 to 0.7. In this calculation several simplifications are made. First, an effect of grain size on M_c magnetization is not considered since the real values of M_c of nanocrystalline alloys are usually smaller as compared to the polycrystalline phase. Values of M_c are additionally reduced due to a presence of Zr

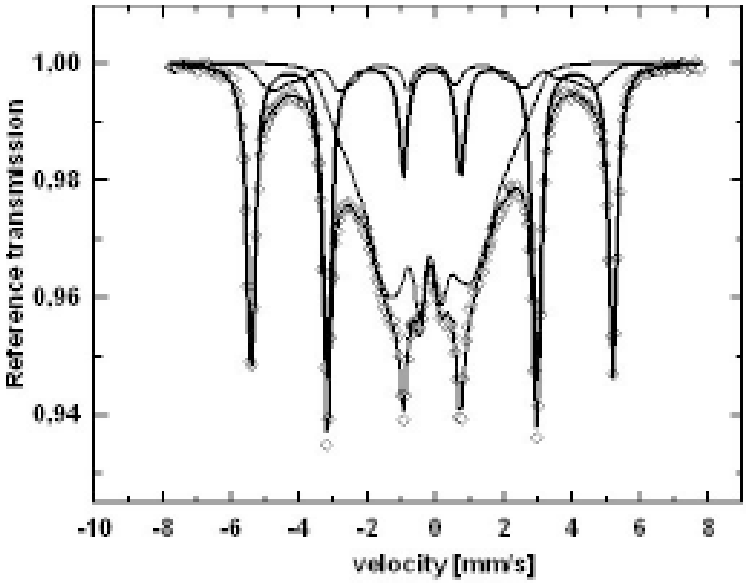

Fig. 3. Mösbauer spectrum of the composite alloy $Fe_{87}Zr_7B_6$ alloy annealed up to 860, 880, 910K.

and B atoms in the bcc - Fe phase. Thus, Eq. (1) underestimates $X(T)$. The abrupt increase in $X(T)$ observed at about 830K may be due to the rapid appearance of the ferromagnetic long range order as well as the relatively high sensitivity of magnetization to crystallization processes.

3.2. Electrical resistivity

The abrupt drop of electrical resistivity at 830 K (Fig. 2) reveals a formation of the bcc Fe (B, Zr) nanocrystals.

We calculate $X(T)$ from Brugmann [8] relation:

$$\frac{(\sigma_a - \sigma)}{(\sigma_a + 2\sigma)}(X-1) = \frac{X(\sigma_c - \sigma)}{(\sigma_c + 2\sigma)}, \qquad (2)$$

where σ_a and σ_c denote the conductivities (equal to $1/\rho_a$ and $1/\rho_c$, respectively) of amorphous and crystalline phases, respectively. σ is a measured conductivity of composite nanocrystalline material consisting of the nanocrystalline phase embedded in the amorphous matrix. Here X describes a volume fraction of the nanocrystalline phase.

For ρ_c we take the value for the bcc Fe phase with grain sizes about 15 nm [9]. Moreover, we neglect an influence of the Zr and B atoms dissolved in the nanocrystalline Fe grains. Nevertheless the Zr and B atoms may enhance the ρ_c resistivity and lead to underestimation of X. For ρ_a the electrical resistivity of the amorphous phase is extrapolated to higher temperatures. Thus we do not take into account the changes of resistivity (probably increasing) due to a transfer of Fe atoms from the amorphous matrix to the nanocrystalline phase. An effect of the grain boundaries composed mainly by Zr layer atoms [5] is also not taken into account. Three oversimplifications listed above act in the same direction underestimating a value of X. Therefore, the derived values of X (Fig. 4) are remarkably lower as compared to other experimental methods applied. It is worth mentioning that systematical error in X related to a roughness of surface samples is large – reaching up to 30%. Thus the total inaccuracy due to the above listed simplifications and systematical errors may become remarkable.

3.3. Mössbauer spectra

The Mössbauer spectra were measured at room temperature for alloys annealed previously above the crystallization threshold temperature T_x up to temperatures Tm**=** 860, 880, and 910K. The recorded Mössbauer spectra of the annealed samples (Fig**.** 3) were fitted in the same way using three magnetic components: (i) a sextet with sharp lines and hyperfine field, H_{hf}, of 32.9 T related to

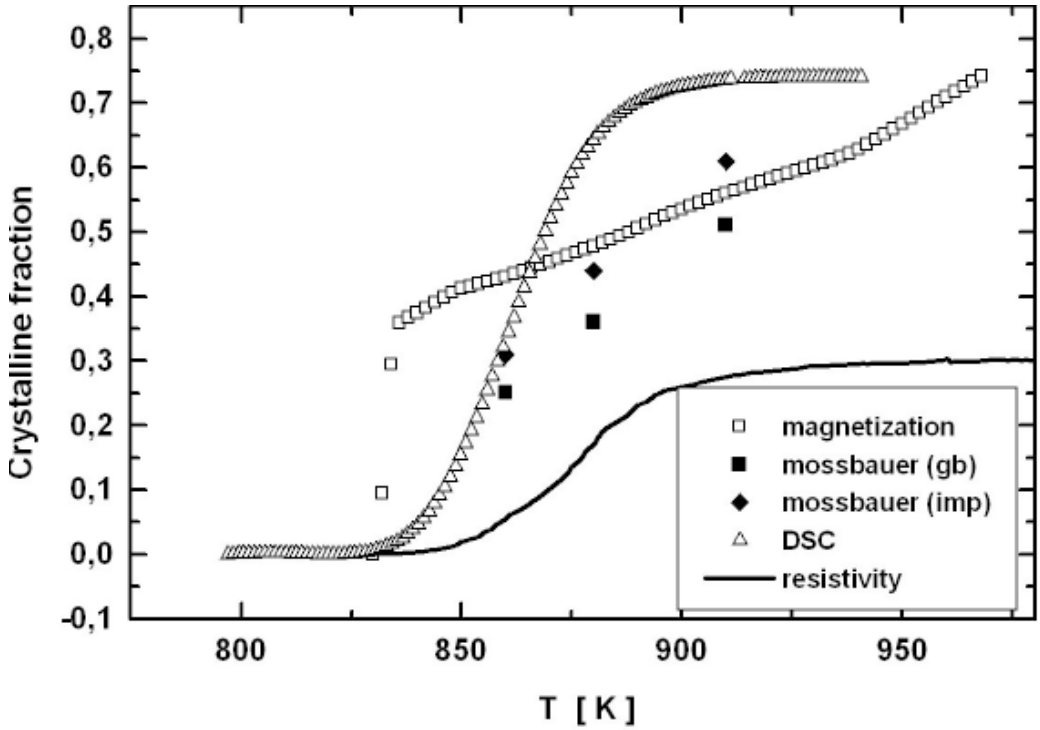

Fig. 4. Temperature variation of crystalline fractions determined by various methods.

the bcc Fe phase, accompanied by (ii) a minor sextet with H_{hf} of about 29.5 T assigned to grain boundary/interface regions, and (iii) a sextet with broadened lines due to hyperfine field distributions originating from the retained amorphous phase (average hyperfine field about 11 T). This fitting approach follows a method proposed by Greneche [10]. The relative abundance of the phases present in the samples was calculated as a ratio of the area of the relevant subspectrum to the total spectral area, assuming similar Debye-Waller factors for each phase.

Since the spectral areas corresponding to three phases I_c, I_a, I_g are proportional to the relative contents of Fe atoms in each phase, then the crystalline fraction X(gb) is determined according to:

$$X = \left(\frac{I_c}{I_c + I_a + I_g} \right) \cdot 0.87. \qquad (3)$$

The relative fraction of the bcc Fe sextet increases with the increase of the annealing temperature indicating the increase of the relative abundance of the nanocrystalline phase at the expense of the amorphous precursor.

For comparision we use also second model proposed by Kemeny [6] in which satellite subspectrum (ii) is not connected with grain boundaries, but with a part of the crystalline phase in which Fe atoms have the B and Zr neighbours. In this case the derived values of X(imp) are about 14% larger as compared to X(gb) (Fig. 4).

The statistical errors of the relative spectral fractions calculated during the fitting procedure of the Mössbauer spectra were ±1%. Moreover, the systematical experimental errors should be also considered since the Mössbauer spectra were recorded in the essentially static mode for samples previously annealed up to temperature Tm, whereas the remaining measurements were performed during a continuous heating.

3.4. Calorimetry

The calorimetric method is based on a proportionality between a mass crystalline fraction and an enthalpy of transition. The crystalline fraction de-

rived from DSC spectrum is plotted in Fig. 4 using a following formula

$$X(T) = \frac{\int_{T_0}^{T} dH}{\int_{T_0}^{T_K} dH}, \quad (4)$$

where T_0 and T_K are temperatures of denote a beginning of the first crystallization stage and the end of the second crystallization stage, respectively.

These values are also subject to systematic errors due to the instability of base line and the neglected variation of amorphous matrix during crystallization. This second factor may be reduced by applying a correction proposed by Barandiaran *et al.* [11], however a final content of the amorphous phase must be known.

4. CONCLUSIONS

The threshold crystallization temperatures determined by the four applied methods remain very close. On the other hand, there is some divergence in values of crystalline fractions originating from the methods applied in this study, which may reflect different sensitivities of each method to structural rearrangements occurring during nanocrystallization. Similar spread in crystalline fractions was also reported by other authors [6,12].

One may notice a relatively good agreement among the X values corresponding to DSC, Mössbauer and magnetization measurements. The most distant values of X derived from electrical resistivity data appeal to consider in more details the roles played by the chemical composition of nanocrystals, grain boundary effects as well as a varying composition of amorphous matrix. Such an analysis will be publish separately [13]. Unfortunately, the XRD data supposed to supply more exact values cannot be analyzed with high enough accuracy due to a high Fe luminescence.

ACKNOWLEDGEMENT

Work supported in part by a grant of Faculty of Physics Warsaw University of Technology. Authors are grateful to Mr. M Fijalkowski for technical assistance.

REFERENCES

[1] E.Pineida, T. Pradell, D. Crespo, N.Clavaguera and M.T Clavaguera-Mora // *J. Non-Crystall. Solids* **287** (2001) 92.
[2] R.M. Ribeiro, D.S. Santos and R.S. Biasi // *J.Alloy Comp*. **363** (2004) 227.
[3] A. Slawska-Waniewska and R. Żuberek // *J. Magn. Magn. Mater* **160** (1996) 253.
[4] K. Suzuki, A. Makino, N. Kataoka, A. Inoue and T. Masumoto // *Mater.Trans. JIM* **32** (1991) 93.
[5] K. Hono // *Prog. Mater. Sci.* **47** (2002) 621.
[6] T. Kemeny, D.A. Kaptas, L.F. Kiss, J. Balogh, I. Vincze, S. Szabo and D.L. Beke // *Hyperfine Interactions* **130** (2000) 181.
[7] B.D. Cullity, In: *Introduction to magnetic materials* (Addison-Wesley Publ. Company, 1972), p. 617.
[8] R. Landauer, In: *Electrical Transport & Optical Properties of Inhomogeneous Media, AIP Conf. Proc. No 40*, ed. by J.C. Garland and D.B. Tanner (AIP, NY 1978), eq 6.5.
[9] C. Martinez-Boubeta, L. Balcels and A. Cebollada // *Appl. Phys. Lett.* **88** (2006) 132511.
[10] J.M. Greneche, N. Randranotoandro, A. Slawska-Waniewska and M. Miglierni // *Hyperfine Interactions* **113** (1998) 279.
[11] J.M. Barandiaran, I. Telleria, J.S. Garitaonandia and H.A. Davies // *J. Non-Crystall. Solids* **329** (2003) 57.
[12] D. Oleszak, A. Grabias, M. Pękala, A. Swiderska-Środa and T. Kulik // *J.All.Comp.* **434-435** (2007) 340.
[13] K. Pekala // *J. Non-Crystall. Solids* **353** (2007) 888.